



ELSEVIER

3 January 2002

PHYSICS LETTERS B

Physics Letters B 524 (2002) 65–80

www.elsevier.com/locate/npe

Search for R-parity violating decays of supersymmetric particles in e^+e^- collisions at LEP

L3 Collaboration

P. Achard^t, O. Adriani^q, M. Aguilar-Benitez^x, J. Alcaraz^{x,r}, G. Alemanni^v, J. Allaby^r,
A. Aloisio^{ab}, M.G. Alviggi^{ab}, H. Anderhub^{au}, V.P. Andreev^{f,ag}, F. Anselmoⁱ,
A. Arefiev^{aa}, T. Azemoon^c, T. Aziz^{j,r}, P. Bagnaia^{al}, A. Bajo^x, G. Baksay^p, L. Baksay^y,
S.V. Baldew^b, S. Banerjee^j, Sw. Banerjee^d, A. Barczyk^{au,as}, R. Barillère^r, P. Bartalini^v,
M. Basileⁱ, N. Batalova^{ar}, R. Battiston^{af}, A. Bay^v, F. Becattini^q, U. Beckerⁿ,
F. Behner^{au}, L. Bellucci^q, R. Berbeco^c, J. Berdugo^x, P. Bergesⁿ, B. Bertucci^{af},
B.L. Betev^{au}, M. Biasini^{af}, M. Biglietti^{ab}, A. Biland^{au}, J.J. Blaising^d, S.C. Blyth^{ah},
G.J. Bobbink^b, A. Böhm^a, L. Boldizar^m, B. Borgia^{al}, S. Bottai^q, D. Bourilkov^{au},
M. Bourquin^t, S. Braccini^t, J.G. Branson^{an}, F. Brochu^d, A. Buijs^{aq}, J.D. Burgerⁿ,
W.J. Burger^{af}, X.D. Caiⁿ, M. Capellⁿ, G. Cara Romeoⁱ, G. Carlino^{ab}, A. Cartacci^q,
J. Casaus^x, F. Cavallari^{al}, N. Cavallo^{ai}, C. Cecchi^{af}, M. Cerrada^x, M. Chamizo^t,
Y.H. Chang^{aw}, M. Chemarin^w, A. Chen^{aw}, G. Chen^g, G.M. Chen^g, H.F. Chen^u,
H.S. Chen^g, G. Chiefari^{ab}, L. Cifarelli^{am}, F. Cindoloⁱ, I. Clareⁿ, R. Clare^{ak},
G. Coignet^d, N. Colino^x, S. Costantini^{al}, B. de la Cruz^x, S. Cucciarelli^{af},
J.A. van Dalen^{ad}, R. de Asmundis^{ab}, P. Déglon^t, J. Debreczeni^m, A. Degré^d,
K. Deiters^{as}, D. della Volpe^{ab}, E. Delmeire^t, P. Denes^{aj}, F. DeNotaristefani^{al},
A. De Salvo^{au}, M. Diemoz^{al}, M. Dierckxsens^b, D. van Dierendonck^b, C. Dionisi^{al},
M. Dittmar^{au,r}, A. Doria^{ab}, M.T. Dova^{k,5}, D. Duchesneau^d, P. Duinker^b, B. Echenard^t,
A. Eline^r, H. El Mamouni^w, A. Engler^{ah}, F.J. Epplingⁿ, A. Ewers^a, P. Extermann^t,
M.A. Falagan^x, S. Falciano^{al}, A. Favara^{ae}, J. Fay^w, O. Fedin^{ag}, M. Felcini^{au},
T. Ferguson^{ah}, H. Fesefeldt^a, E. Fiandrini^{af}, J.H. Field^t, F. Filthaut^{ad}, P.H. Fisherⁿ,
W. Fisher^{aj}, I. Fisk^{an}, G. Forconiⁿ, K. Freudenreich^{au}, C. Furetta^z, Yu. Galaktionov^{aa,n},
S.N. Ganguli^j, P. Garcia-Abia^{e,r}, M. Gataullin^{ae}, S. Gentile^{al}, S. Giagu^{al}, Z.F. Gong^u,
G. Grenier^w, O. Grimm^{au}, M.W. Gruenewald^{h,a}, M. Guida^{am}, R. van Gulik^b,
V.K. Gupta^{aj}, A. Gurtu^j, L.J. Gutay^{ar}, D. Haas^e, D. Hatzifotiadouⁱ, T. Hebbeker^{h,a},
A. Hervé^r, J. Hirschfelder^{ah}, H. Hofer^{au}, M. Hohmann^y, G. Holzner^{au}, S.R. Hou^{aw},
Y. Hu^{ad}, B.N. Jin^g, L.W. Jones^c, P. de Jong^b, I. Josa-Mutuberría^x, D. Käfer^a,
M. Kaur^o, M.N. Kienzle-Focacci^t, J.K. Kim^{ap}, J. Kirkby^r, W. Kittel^{ad},
A. Klimentov^{n,aa}, A.C. König^{ad}, M. Kopal^{ar}, V. Koutsenko^{n,aa}, M. Kräber^{au},

R.W. Kraemer^{ah}, W. Krenz^a, A. Krüger^{at}, A. Kunin^{n,an,aa}, P. Ladron de Guevara^x, I. Laktineh^w, G. Landi^q, M. Lebeau^r, A. Lebedevⁿ, P. Lebrun^w, P. Lecomte^{au}, P. Lecoq^r, P. Le Coultre^{au}, J.M. Le Goff^r, R. Leiste^{at}, P. Levchenko^{ag}, C. Li^u, S. Likhoded^{at}, C.H. Lin^{aw}, W.T. Lin^{aw}, F.L. Linde^b, L. Lista^{ab}, Z.A. Liu^g, W. Lohmann^{at}, E. Longo^{al}, Y.S. Lu^g, K. Lübelmeyer^a, C. Luci^{al}, L. Luminari^{al}, W. Lustermaun^{au}, W.G. Ma^u, L. Malgeri^t, A. Malinin^{aa}, C. Maña^x, D. Mangeol^{ad}, J. Mans^{aj}, J.P. Martin^w, F. Marzano^{al}, K. Mazumdar^j, R.R. McNeil^f, S. Mele^{r,ab}, L. Merola^{ab}, M. Meschini^q, W.J. Metzger^{ad}, A. Mihul^l, H. Milcent^r, G. Mirabelli^{al}, J. Mnich^a, G.B. Mohanty^j, G.S. Muanza^w, A.J.M. Muijs^b, B. Musicar^{an}, M. Musy^{al}, S. Nagy^p, S. Natale^t, M. Napolitano^{ab}, F. Nessi-Tedaldi^{au}, H. Newman^{ae}, T. Niessen^a, A. Nisati^{al}, H. Nowak^{at}, R. Ofierzynski^{au}, G. Organtini^{al}, C. Palomares^r, D. Pandoulas^a, P. Paolucci^{ab}, R. Paramatti^{al}, G. Passaleva^q, S. Patricelli^{ab}, T. Paul^k, M. Pauluzzi^{af}, C. Pausⁿ, F. Pauss^{au}, M. Pedace^{al}, S. Pensotti^z, D. Perret-Gallix^d, B. Petersen^{ad}, D. Piccolo^{ab}, F. Pierellaⁱ, M. Pioppi^{af}, P.A. Piroué^{aj}, E. Pistolesi^z, V. Plyaskin^{aa}, M. Pohl^t, V. Pojidaev^q, J. Pothier^r, D.O. Prokofiev^{ar}, D. Prokofiev^{ag}, J. Quartieri^{am}, G. Rahal-Callot^{au}, M.A. Rahaman^j, P. Raics^p, N. Raja^j, R. Ramelli^{au}, P.G. Rancoita^z, R. Ranieri^q, A. Raspereza^{at}, P. Razis^{ac}, D. Ren^{au}, M. Rescigno^{al}, S. Reucroft^k, S. Riemann^{at}, K. Riles^c, B.P. Roe^c, L. Romero^x, A. Rosca^h, S. Rosier-Lees^d, S. Roth^a, C. Rosenbleck^a, B. Roux^{ad}, J.A. Rubio^r, G. Ruggiero^q, H. Rykaczewski^{au}, A. Sakharov^{au}, S. Saremi^f, S. Sarkar^{al}, J. Salicio^r, E. Sanchez^x, M.P. Sanders^{ad}, C. Schäfer^r, V. Schegelsky^{ag}, S. Schmidt-Kaerst^a, D. Schmitz^a, H. Schopper^{av}, D.J. Schotanus^{ad}, G. Schwering^a, C. Sciacca^{ab}, L. Servoli^{af}, S. Shevchenko^{ae}, N. Shivarov^{ao}, V. Shoutko^{aa,an,n}, E. Shumilov^{aa}, A. Shvorob^{ae}, T. Siedenburg^a, D. Son^{ap}, P. Spillantini^q, M. Steuerⁿ, D.P. Stickland^{aj}, B. Stoyanov^{ao}, A. Straessner^r, K. Sudhakar^j, G. Sultanov^{ao}, L.Z. Sun^u, S. Sushkov^h, H. Suter^{au}, J.D. Swain^k, Z. Szillasi^{y,3}, X.W. Tang^g, P. Tarjan^p, L. Tauscher^e, L. Taylor^k, B. Tellili^w, D. Teyssier^w, C. Timmermans^{ad}, Samuel C.C. Tingⁿ, S.M. Tingⁿ, S.C. Tonwar^{j,r}, J. Tóth^m, C. Tully^{aj}, K.L. Tung^g, J. Ulbricht^{au}, E. Valente^{al}, R.T. Van de Walle^{ad}, V. Veszpremi^y, G. Vesztergombi^m, I. Vetlitsky^{aa}, D. Vicinanza^{am}, G. Viertel^{au}, S. Villa^{ak}, M. Vivargent^d, S. Vlachos^e, I. Vodopianov^{ag}, H. Vogel^{ah}, H. Vogt^{at}, I. Vorobiev^{ah,aa}, A.A. Vorobyov^{ag}, M. Wadhwa^e, W. Wallraff^a, X.L. Wang^u, Z.M. Wang^u, M. Weber^a, P. Wienemann^a, H. Wilkens^{ad}, S. Wynhoff^{aj}, L. Xia^{ae}, Z.Z. Xu^u, J. Yamamoto^c, B.Z. Yang^u, C.G. Yang^g, H.J. Yang^c, M. Yang^g, S.C. Yeh^{ax}, An. Zalite^{ag}, Yu. Zalite^{ag}, Z.P. Zhang^u, J. Zhao^u, G.Y. Zhu^g, R.Y. Zhu^{ae}, H.L. Zhuang^g, A. Zichichi^{i,r,s}, G. Zilizi^{y,3}, B. Zimmermann^{au}, M. Zöller^a

^a I. Physikalisches Institut, RWTH, D-52056 Aachen, Germany¹,
III. Physikalisches Institut, RWTH, D-52056 Aachen, Germany¹

^b National Institute for High Energy Physics, NIKHEF, and University of Amsterdam, NL-1009 DB Amsterdam, The Netherlands

^c University of Michigan, Ann Arbor, MI 48109, USA

- ^d Laboratoire d'Annecy-le-Vieux de Physique des Particules, LAPP, IN2P3-CNRS, BP 110, F-74941 Annecy-le-Vieux Cedex, France
- ^e Institute of Physics, University of Basel, CH-4056 Basel, Switzerland
- ^f Louisiana State University, Baton Rouge, LA 70803, USA
- ^g Institute of High Energy Physics, IHEP, 100039 Beijing, PR China ⁶
- ^h Humboldt University, D-10099 Berlin, Germany ¹
- ⁱ University of Bologna, and INFN, Sezione di Bologna, I-40126 Bologna, Italy
- ^j Tata Institute of Fundamental Research, Mumbai (Bombay) 400 005, India
- ^k Northeastern University, Boston, MA 02115, USA
- ^l Institute of Atomic Physics and University of Bucharest, R-76900 Bucharest, Romania
- ^m Central Research Institute for Physics of the Hungarian Academy of Sciences, H-1525 Budapest 114, Hungary ²
- ⁿ Massachusetts Institute of Technology, Cambridge, MA 02139, USA
- ^o Panjab University, Chandigarh 160 014, India
- ^p KLTE-ATOMKI, H-4010 Debrecen, Hungary ³
- ^q INFN, Sezione di Firenze, and University of Florence, I-50125 Florence, Italy
- ^r European Laboratory for Particle Physics, CERN, CH-1211 Geneva 23, Switzerland
- ^s World Laboratory, FBLJA Project, CH-1211 Geneva 23, Switzerland
- ^t University of Geneva, CH-1211 Geneva 4, Switzerland
- ^u Chinese University of Science and Technology, USTC, Hefei, Anhui 230 029, PR China ⁶
- ^v University of Lausanne, CH-1015 Lausanne, Switzerland
- ^w Institut de Physique Nucléaire de Lyon, IN2P3-CNRS, Université Claude Bernard, F-69622 Villeurbanne, France
- ^x Centro de Investigaciones Energéticas, Medioambientales y Tecnológicas, CIEMAT, E-28040 Madrid, Spain ⁴
- ^y Florida Institute of Technology, Melbourne, FL 32901, USA
- ^z INFN, Sezione di Milano, I-20133 Milan, Italy
- ^{aa} Institute of Theoretical and Experimental Physics, ITEP, Moscow, Russia
- ^{ab} INFN, Sezione di Napoli, and University of Naples, I-80125 Naples, Italy
- ^{ac} Department of Physics, University of Cyprus, Nicosia, Cyprus
- ^{ad} University of Nijmegen and NIKHEF, NL-6525 ED Nijmegen, The Netherlands
- ^{ae} California Institute of Technology, Pasadena, CA 91125, USA
- ^{af} INFN, Sezione di Perugia, and Università Degli Studi di Perugia, I-06100 Perugia, Italy
- ^{ag} Nuclear Physics Institute, St. Petersburg, Russia
- ^{ah} Carnegie Mellon University, Pittsburgh, PA 15213, USA
- ^{ai} INFN, Sezione di Napoli, and University of Potenza, I-85100 Potenza, Italy
- ^{aj} Princeton University, Princeton, NJ 08544, USA
- ^{ak} University of California, Riverside, CA 92521, USA
- ^{al} INFN, Sezione di Roma, and University of Rome "La Sapienza", I-00185 Rome, Italy
- ^{am} University and INFN, Salerno, I-84100 Salerno, Italy
- ^{an} University of California, San Diego, CA 92093, USA
- ^{ao} Bulgarian Academy of Sciences, Central Laboratory of Mechatronics and Instrumentation, BU-1113 Sofia, Bulgaria
- ^{ap} The Center for High Energy Physics, Kyungpook National University, 702-701 Taegu, South Korea
- ^{aq} Utrecht University and NIKHEF, NL-3584 CB Utrecht, The Netherlands
- ^{ar} Purdue University, West Lafayette, IN 47907, USA
- ^{as} Paul Scherrer Institut, PSI, CH-5232 Villigen, Switzerland
- ^{at} DESY, D-15738 Zeuthen, Germany
- ^{au} Eidgenössische Technische Hochschule, ETH Zürich, CH-8093 Zürich, Switzerland
- ^{av} University of Hamburg, D-22761 Hamburg, Germany
- ^{aw} National Central University, Chung-Li, Taiwan, ROC
- ^{ax} Department of Physics, National Tsing Hua University, Taiwan, ROC

Abstract

A search, in e^+e^- collisions, for chargino, neutralino, scalar lepton and scalar quark pair-production is performed, without assuming R -parity conservation in decays, in the case that only one of the coupling constants λ or λ'' is non-negligible. No signal is found in data up to a centre-of-mass energy of 208 GeV. Limits on the production cross sections and on the masses of supersymmetric particles are derived. © 2002 Elsevier Science B.V. All rights reserved.

1. Introduction

The most general superpotential of the Minimal Supersymmetric Standard Model (MSSM) [1], which describes a supersymmetric, renormalizable and gauge-invariant theory, with minimal particle content, includes the term W_R [2,3]:

$$W_R = \lambda_{ijk} L_i L_j \bar{E}_k + \lambda'_{ijk} L_i Q_j \bar{D}_k + \lambda''_{ijk} \bar{U}_i \bar{D}_j \bar{D}_k, \quad (1)$$

where λ_{ijk} , λ'_{ijk} and λ''_{ijk} denote the Yukawa couplings and i , j and k the generation indices; L_i and Q_i are the left-handed lepton- and quark-doublet superfields, \bar{E}_i , \bar{D}_i and \bar{U}_i are the right-handed singlet superfields for charged leptons, down- and up-type quarks, respectively. The $L_i L_j \bar{E}_k$ and $L_i Q_j \bar{D}_k$ terms violate the leptonic quantum number L , while the $\bar{U}_i \bar{D}_j \bar{D}_k$ terms violate the baryonic quantum number B .

R -parity is a multiplicative quantum number defined as:

$$R = (-1)^{3B+L+2S}, \quad (2)$$

where S is the spin. For ordinary particles R is $+1$, while it is -1 for their supersymmetric partners. R -parity conservation implies that supersymmet-

ric particles can only be produced in pairs and then decay in cascade to the lightest supersymmetric particle (LSP), which is stable [4]. This hypothesis is formulated in order to prevent a fast proton decay [5], disfavoured by present limits [6]. However, the absence of either the B - or the L -violating terms is enough to prevent such a decay, and the hypothesis of R -parity conservation can be relaxed. As a consequence, two new kinds of processes are allowed: single production of supersymmetric particles [7,8], or LSP decays into Standard Model particles via scalar lepton or scalar quark exchange. For these decays, the MSSM production mechanisms are unaltered by the operators in Eq. (1). In this Letter the cases in which either a neutralino or a scalar lepton is the LSP are considered.

In this Letter we describe the search for pair-produced neutralinos ($e^+e^- \rightarrow \tilde{\chi}_m^0 \tilde{\chi}_n^0$, with $m = 1, 2$ and $n = 1, \dots, 4$), charginos ($e^+e^- \rightarrow \tilde{\chi}_1^+ \tilde{\chi}_1^-$), scalar leptons ($e^+e^- \rightarrow \tilde{\ell}_R^+ \tilde{\ell}_R^-$, where $\tilde{\ell}_R^\pm$ represents scalar electrons, muons or tau and $e^+e^- \rightarrow \tilde{\nu} \tilde{\nu}$) and scalar quarks ($e^+e^- \rightarrow \tilde{q} \tilde{q}$) with subsequent R -parity violating decays, assuming that only one of the coupling constants λ_{ijk} or λ'_{ijk} is non-negligible. Only the supersymmetric partners of the right-handed charged leptons, $\tilde{\ell}_R$, are considered, as they are expected to be lighter than the corresponding left-handed ones.

Supersymmetric particles can either decay directly into two or three fermions according to the dominant interaction term, or indirectly via the LSP. The different decay modes are detailed in Table 1. Four-body decays of the lightest scalar lepton are also taken into account in the case of λ''_{ijk} . In the present analysis, the dominant coupling is assumed to be greater than 10^{-5} [9], which corresponds to decay lengths below 1 cm.

Previous L3 results at centre-of-mass energies (\sqrt{s}) up to 189 GeV are reported in Refs. [10] and [11],

¹ Supported by the German Bundesministerium für Bildung, Wissenschaft, Forschung und Technologie.

² Supported by the Hungarian OTKA fund under contract numbers T019181, F023259 and T024011.

³ Also supported by the Hungarian OTKA fund under contract number T026178.

⁴ Supported also by the Comisión Interministerial de Ciencia y Tecnología.

⁵ Also supported by CONICET and Universidad Nacional de La Plata, CC 67, 1900 La Plata, Argentina.

⁶ Supported by the National Natural Science Foundation of China.

Table 1

R -parity violating decays of the supersymmetric particles considered in this analysis. Charged conjugate states are implied. Indirect decays via scalar leptons are relevant only for neutralinos when the scalar lepton is the LSP. Only supersymmetric partners of the right-handed charged leptons are taken into account. Decays to more than three fermions are not listed. Z^* and W^* indicate virtual Z and W bosons

Particle	Direct decays		Indirect decays	
	λ_{ijk}	λ''_{ijk}	via $\tilde{\chi}_1^0$	via $\tilde{\ell}$
$\tilde{\chi}_1^0$	$\ell_i^- \nu_j \ell_k^+, \nu_i \ell_j^+ \ell_k^-$	$\bar{u}_i \bar{d}_j \bar{d}_k$	–	$\ell \bar{\ell}$
$\tilde{\chi}_n^0 (n \geq 2)$	$\ell_i^- \nu_j \ell_k^+, \nu_i \ell_j^+ \ell_k^-$	$\bar{u}_i \bar{d}_j \bar{d}_k$	$Z^* \tilde{\chi}_m^0 (m < n),$ $W^* \tilde{\chi}_1^\pm$	$\ell \bar{\ell}$
$\tilde{\chi}_1^+$	$\nu_i \nu_j \ell_k^+, \ell_i^+ \ell_j^+ \ell_k^-$	$\bar{d}_i \bar{d}_j \bar{d}_k, u_i u_j d_k,$ $u_i d_j u_k$	$W^* \tilde{\chi}_1^0, W^* \tilde{\chi}_2^0$	–
$\tilde{\ell}_{kR}^-$	$\nu_i \ell_j^-, \nu_j \ell_i^-$	–	$\ell_k^- \tilde{\chi}_1^0$	–
$\tilde{\nu}_i, \tilde{\nu}_j$	$\ell_j^- \ell_k^+, \ell_i^- \ell_k^+$	–	$\nu_i \tilde{\chi}_1^0, \nu_j \tilde{\chi}_1^0$	–
\bar{u}_{iR}	–	$\bar{d}_j \bar{d}_k$	$u_i \tilde{\chi}_1^0$	–
$\bar{d}_{jR}, \bar{d}_{kR}$	–	$\bar{u}_i \bar{d}_k, \bar{u}_i \bar{d}_j$	$d_j \tilde{\chi}_1^0, d_k \tilde{\chi}_1^0$	–

where also λ'_{ijk} couplings are discussed. Two new analyses are presented in this letter: $e^+e^- \rightarrow \tilde{\nu}\tilde{\nu}$ and $e^+e^- \rightarrow \tilde{q}\tilde{q}$ in the case of λ''_{ijk} couplings. New interpretations for scalar leptons and scalar quarks in the MSSM framework are also performed.

Searches for R -parity violating decays of supersymmetric particles were also reported by other LEP experiments [8,12].

2. Data and Monte Carlo samples

The data used correspond to an integrated luminosity of 450.6 pb^{-1} collected with the L3 detector [13] at $\sqrt{s} = 192\text{--}208 \text{ GeV}$. For the search for scalar quarks and scalar neutrinos decaying via λ''_{ijk} couplings, also the data sample collected at $\sqrt{s} = 189 \text{ GeV}$ is used. This corresponds to an additional integrated luminosity of 176.4 pb^{-1} .

The signal events are generated with the program SUSYGEN [14] for different mass values and for all possible choices of the generation indices.

The following Monte Carlo generators are used to simulate Standard Model background processes: PYTHIA [15] for $e^+e^- \rightarrow Ze^+e^-$ and $e^+e^- \rightarrow$

ZZ , BHWIDE [16] for $e^+e^- \rightarrow e^+e^-$, KK2F [17] for $e^+e^- \rightarrow \mu^+\mu^-$, $e^+e^- \rightarrow \tau^+\tau^-$ and $e^+e^- \rightarrow q\bar{q}$, PHOJET [18] and PYTHIA for $e^+e^- \rightarrow e^+e^-$ hadrons, DIAG36 [19] for $e^+e^- \rightarrow e^+e^-\ell^+\ell^-$ ($\ell = e, \mu, \tau$), KORALW [20] for $e^+e^- \rightarrow W^+W^-$ and EXCALIBUR [21] for $e^+e^- \rightarrow q\bar{q}'\ell\nu$ and $e^+e^- \rightarrow \ell\nu\ell'\nu$. The number of simulated events corresponds to at least 50 times the luminosity of the data, except for Bhabha and two-photon processes, where the Monte Carlo samples correspond to 2 to 10 times the luminosity.

The detector response is simulated using the GEANT package [22]. It takes into account effects of energy loss, multiple scattering and showering in the detector materials. Hadronic interactions are simulated with the GHEISHA program [23]. Time-dependent detector inefficiencies are also taken into account in the simulation procedure.

Data and Monte Carlo samples are reconstructed with the same program. Isolated leptons ($\ell = e, \mu, \tau$) are identified as described in Ref. [11]. Remaining clusters and tracks are classified as hadrons. Jets are reconstructed with the DURHAM algorithm [24]. The jet resolution parameter y_{mn} is defined as the y_{cut} value at which the event configuration changes from n to m

jets. At least one time of flight measurement has to be consistent with the beam crossing to reject cosmic rays.

3. λ_{ijk} analysis

The different topologies arising when λ_{ijk} couplings dominate are shown in Table 2 and can be classified into four categories: $2\ell + \cancel{E}$, $4\ell + \cancel{E}$, 6ℓ , $\geq 4\ell$ plus possible jets and \cancel{E} . The missing energy \cancel{E} indicates final state neutrinos escaping detection. After a common preselection [11], based on the visible energy, the event multiplicity and the number of identified leptons, a dedicated selection is developed for each group, taking into account lepton flavours, particle boosts and virtual W and Z decay products.

After the preselection is applied, 2567 events are selected in the data sample and 2593 ± 12 events are expected from Standard Model processes. The main contributions are: 44.5% from W^+W^- , 21.5% from $q\bar{q}$, 14.7% from $q\bar{q}'e\nu$, 6.6% from two-photon processes (3.9% from $e^+e^-e^+e^-$ and 2.7% from e^+e^- hadrons), and 5.6% from $\tau^+\tau^-$ events.

Fig. 1 shows the distributions of the number of leptons, thrust, normalised visible energy and $\ln(\gamma_{34})$

Table 2

Processes considered in the λ_{ijk} analysis and corresponding selections [11]. $\tilde{\chi}_m^0 \tilde{\chi}_n^0$ indicates neutralino pair-production with $m = 1, 2$ and $n = 1, \dots, 4$. ‘‘Cascades’’ refers to all possible final state combinations of Table 1

Direct decays		Selections
$e^+e^- \rightarrow \tilde{\chi}_m^0 \tilde{\chi}_n^0 \rightarrow$	$llll\nu\nu$	$4\ell + \cancel{E}$
$e^+e^- \rightarrow \tilde{\chi}_1^+ \tilde{\chi}_1^- \rightarrow$	$llllll$	6ℓ
	$llll\nu\nu$	$4\ell + \cancel{E}$
	$ll\nu\nu\nu\nu$	$2\ell + \cancel{E}$
$e^+e^- \rightarrow \tilde{\ell}_R^+ \tilde{\ell}_R^- \rightarrow$	$lv\nu\nu$	$2\ell + \cancel{E}$
$e^+e^- \rightarrow \tilde{\nu}\tilde{\nu} \rightarrow$	$llll$	$4\ell + \cancel{E}$
Indirect decays		Selections
$e^+e^- \rightarrow \tilde{\chi}_m^0 \tilde{\chi}_{n(n \geq 2)}^0 \rightarrow$	cascades	$\geq 4\ell + (\text{jets}) + \cancel{E}$
$e^+e^- \rightarrow \tilde{\chi}_1^+ \tilde{\chi}_1^- \rightarrow$	$\tilde{\chi}_{1(2)}^0 \tilde{\chi}_{1(2)}^0 W^*W^*$	$\geq 4\ell + (\text{jets}) + \cancel{E}$
$e^+e^- \rightarrow \tilde{\ell}_R^+ \tilde{\ell}_R^- \rightarrow$	$llllll\nu\nu$	$\geq 4\ell + (\text{jets}) + \cancel{E}$
$e^+e^- \rightarrow \tilde{\nu}\tilde{\nu} \rightarrow$	$llll\nu\nu\nu\nu$	$4\ell + \cancel{E}$

after the preselection. The data are in good agreement with the Monte Carlo expectations.

The final selection criteria are discussed in Ref. [11] and yield the efficiencies for direct and indirect decays of the supersymmetric particles summarized in Tables 3 and 4, respectively. Here and in the following sections we discuss only the results obtained for those choices of the generation indices which give the lowest selection efficiencies. The quoted results will thus be conservatively valid for any ijk combination. In the case of direct R -parity violating decays, the efficiencies are estimated for different mass values of the pair-produced supersymmetric particles. In the case of indirect decays, the efficiencies are estimated for different masses and ΔM ranges. ΔM is defined as the mass difference $M_{\text{susy}} - M_{\tilde{\chi}_1^0}$, where M_{susy} is the mass of the supersymmetric particle under investigation.

For direct neutralino or chargino decays, as well as for all indirect decays studied, the lowest efficiencies are found for $\lambda_{ijk} = \lambda_{133}$, due to the presence in the final state of taus, whose detection is more difficult.

In the case of pair-production of scalar charged leptons, followed by direct decays via λ_{ijk} , the final state contains two leptons plus missing energy. The lepton flavours are given by the indices i and j , independently of the value of k . The lowest selection efficiency is found for $\lambda_{ijk} = \lambda_{12k}$, i.e., for events with electrons and muons in the final state, since these low multiplicity events require a tight selection to suppress the large background from lepton pair-production.

Direct decays of scalar neutrinos yield four leptons in the final state. The $4\ell + \cancel{E}$ selections are used as they provide a good analysis sensitivity comparable to that of the dedicated selections for scalar electrons, muons and taus. Scalar neutrino decays into electrons and muons are selected with lower efficiency than decays into taus, due to the missing energy requirements. In particular, the lowest efficiency is obtained for λ_{121} , which can give rise to the decays $\tilde{\nu}_e \rightarrow \mu^- e^+$ and $\tilde{\nu}_\mu \rightarrow e^- e^+$.

4. λ''_{ijk} analysis

When the λ''_{ijk} couplings dominate, the flavour composition depends on the generation indices. In the case of neutralino and chargino pair-production,

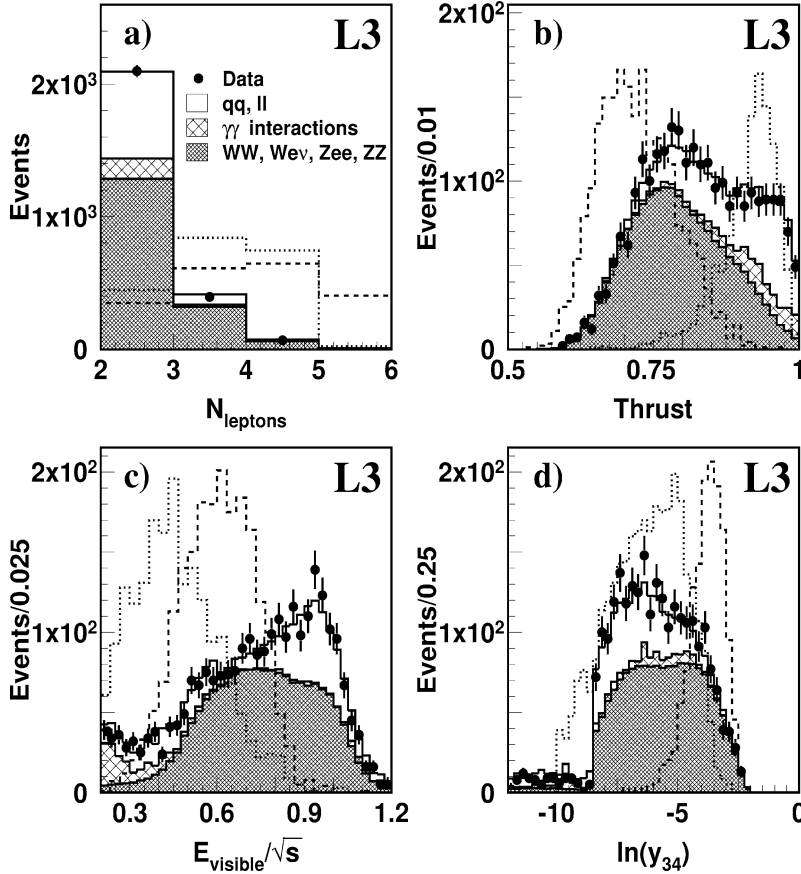


Fig. 1. Data and Monte Carlo distributions of (a) the number of leptons, (b) thrust, (c) the normalised visible energy and (d) $\ln(y_{34})$ after the λ_{ijk} preselection. The solid histograms show the expectations for Standard Model processes. The dotted and dashed histograms show two examples of signal, with dominant coupling λ_{133} . The dotted histograms represent the process $e^+e^- \rightarrow \tilde{\chi}_1^0 \tilde{\chi}_1^0$, for $M_{\tilde{\chi}_1^0} = 42$ GeV, corresponding to two hundred times the luminosity of the data. The dashed ones represent $e^+e^- \rightarrow \tilde{\chi}_1^+ \tilde{\chi}_1^-$, with $M_{\tilde{\chi}_1^\pm} = 92$ GeV and $\Delta M = M_{\tilde{\chi}_1^\pm} - M_{\tilde{\chi}_1^0} = 50$ GeV, corresponding to twenty times this luminosity.

the different topologies can be classified into two groups: multijets and multijets with leptons and/or missing energy, as shown in Table 5. After a common preselection [11], dedicated selections are developed for each group, depending on the particle boosts, the ΔM values and the virtual W decay products.

In the case of neutralino, chargino, scalar charged lepton and scalar quark pair-production, the preselection aims at selecting well balanced hadronic events and yields 11770 events in the data sample to be compared with 11719 ± 31 expected from Standard Model processes, of which 62.0% are from $q\bar{q}$ and 32.8% W^+W^- . Fig. 2 shows the distributions of thrust,

$\ln(y_{34})$, $\ln(y_{45})$ and width of the most energetic jet after the preselection. The width of a jet is defined as $p_T^{\text{jet}}/E^{\text{jet}}$, where the event is clustered into exactly two jets, and p_T^{jet} is the sum of the projections of the particle momenta on to a plane perpendicular to the jet axis, and E^{jet} is the jet energy. There is good agreement between data and Monte Carlo expectations. The efficiencies for direct and indirect decays of the supersymmetric particles after the selections discussed in Ref. [11] are summarized in Tables 3 and 4, respectively.

Scalar quarks and scalar neutrinos, not studied in our previous papers, are searched for as follows. Scalar

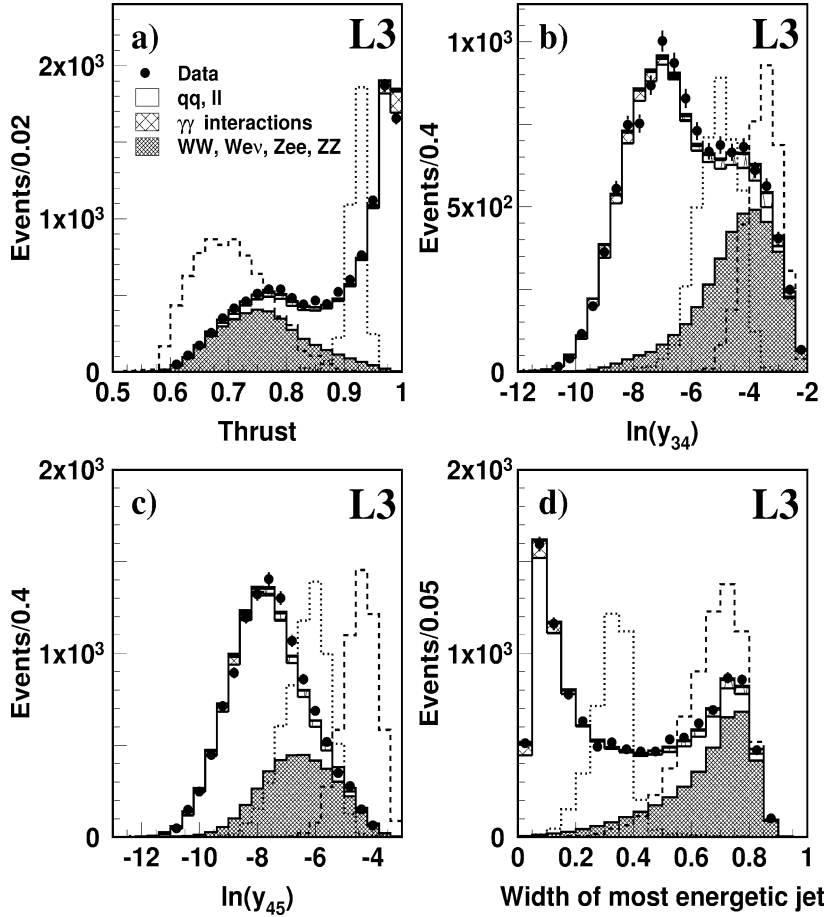


Fig. 2. Data and Monte Carlo distributions of (a) thrust, (b) $\ln(y_{34})$, (c) $\ln(y_{45})$ and (d) width of the most energetic jet after the λ''_{ijk} preselection. The solid histograms show the expectations for Standard Model processes. The dashed and dotted histograms show two examples of signal, with dominant coupling λ''_{212} , corresponding to decays into c , d and s quarks. The dotted histograms represent the process $e^+e^- \rightarrow \tilde{\chi}_1^0 \tilde{\chi}_1^0$, with $M_{\tilde{\chi}_1^0} = 40$ GeV, corresponding to one hundred times the luminosity of the data. The dashed ones represent $e^+e^- \rightarrow \tilde{\chi}_1^+ \tilde{\chi}_1^-$, with $M_{\tilde{\chi}_1^\pm} = 90$ GeV and $\Delta M = M_{\tilde{\chi}_1^\pm} - M_{\tilde{\chi}_1^0} = 60$ GeV, corresponding to fifteen times this luminosity.

quark pairs can decay directly into 4 or indirectly into 8 quarks, as shown in Table 1. In the first case, the main background sources are $q\bar{q}$ events and W^+W^- decays. For low masses of the primary scalar quarks, the signal configuration is more similar to two back-to-back jets, due to the large jet boost. In this case we use the least energetic jet width to reject the $q\bar{q}$ background, which is the dominant one at low masses. For larger scalar quark masses ($M_{\tilde{q}} > 50$ GeV), the signal events are better described by a 4-jet configuration and selection criteria are applied on y_{34} and the χ^2 of a kinematical fit, which imposes four-

momentum conservation and equal mass constraints. In the case of indirect decays into 8 quarks, the same selections as for $\tilde{\chi}_1^0 \tilde{\chi}_1^0$ decays into 6 quarks are used [11].

For scalar neutrino pair-production, a different preselection is performed, to take into account the missing momentum in the final state. Low multiplicity events, such as leptonic Z and W decays, are rejected by requiring at least 13 calorimetric clusters. At least one charged track has to be present. The visible energy has to be greater than $0.2\sqrt{s}$. In order to remove background contributions from two-photon interactions,

Table 3

Efficiency values (ϵ , in %) and 95% C.L. cross section upper limits (σ , in pb) for direct decays of the supersymmetric particles, as a function of their mass (M , in GeV). As an example the efficiencies at $\sqrt{s} = 206$ GeV are shown, for the most conservative choice of the couplings. At the other centre-of-mass energies they are compatible within the uncertainties. Typical relative errors on the signal efficiencies, due to Monte Carlo statistics, are between 2% and 5%. $\tilde{\chi}_m^0 \tilde{\chi}_n^0$ indicates neutralino pair-production with $m = 1, 2$ and $n = 1, \dots, 4$. For direct neutralino decays we quote the $\tilde{\chi}_1^0 \tilde{\chi}_1^0$ efficiencies. The upper limits on the pair-production cross sections are calculated using the full data sample, with a total luminosity of 627 pb^{-1} , except for the last mass point, where only the data collected at $\sqrt{s} \geq 204$ GeV are used, corresponding to a luminosity of 216 pb^{-1} . Chargino and scalar lepton pair-production via λ_{ijk} couplings are not investigated for mass values excluded in Ref. [11]. For the processes marked with * we refer to four-body decays, as described in Section 4

Coupling	Process		M							
			30	40	50	60	70	80	90	102
<i>Direct decays</i>										
λ_{133}	$\tilde{\chi}_m^0 \tilde{\chi}_n^0$	ϵ	15	24	32	37	40	42	45	46
		σ	0.07	0.05	0.04	0.03	0.03	0.03	0.02	0.07
λ_{133}	$\tilde{\chi}_1^+ \tilde{\chi}_1^-$	ϵ	–	–	–	–	38	40	43	43
		σ	–	–	–	–	0.07	0.06	0.06	0.17
λ_{12k}	$\tilde{\ell}_R^+ \tilde{\ell}_R^-$	ϵ	–	–	–	–	6	6	8	6
		σ	–	–	–	–	0.39	0.36	0.27	1.16
λ_{121}	$\tilde{\nu} \tilde{\nu}$	ϵ	–	–	–	–	6	8	7	5
		σ	–	–	–	–	0.20	0.15	0.17	0.68
λ'_{212}	$\tilde{\chi}_m^0 \tilde{\chi}_n^0, \tilde{\chi}_1^+ \tilde{\chi}_1^-$	ϵ	39	49	40	44	42	43	46	56
		σ	0.11	0.10	0.08	0.12	0.12	0.11	0.10	0.18
λ'_{212}	$\tilde{e}_R^+ \tilde{e}_R^- *$, $\tilde{\mu}_R^+ \tilde{\mu}_R^- *$	ϵ	39	49	40	44	42	43	46	56
		σ	0.11	0.10	0.08	0.12	0.12	0.11	0.10	0.18
λ'_{212}	$\tilde{\tau}_R^+ \tilde{\tau}_R^- *$	ϵ	39	49	38	44	42	19	14	13
		σ	0.11	0.10	0.15	0.12	0.11	0.18	0.22	0.28
λ'_{212}	$\tilde{\nu} \tilde{\nu} *$	ϵ	7	14	29	21	21	22	25	56
		σ	0.66	0.16	0.13	0.18	0.18	0.17	0.15	0.18
λ'_{212}	$\tilde{q} \tilde{q}$	ϵ	27	26	22	32	31	34	34	34
		σ	0.10	0.13	0.07	0.05	0.28	0.27	0.16	0.13

the energy in a cone of 12° half-opening angle around the beam axis has to be below 20% of the total visible energy. Furthermore, the thrust axis is required to be well contained in the detector. Unbalanced events with an initial state radiation photon in the beam pipe are removed. Semileptonic W^+W^- decays are rejected by the requirement that neither the dijet invariant mass nor that of any identified lepton and the missing four-momentum should be in a 5 GeV interval around the W mass. This preselection yields 13 950 events in the data at $\sqrt{s} = 189\text{--}208$ GeV where 13662 ± 45 are expected from Standard Model processes and the main contributions are 50.6% from $q\bar{q}$, 32.8% from W^+W^- ,

9.2% from $e^+e^-q\bar{q}$ and 4.0% from $q\bar{q}'e\nu$. The difference in the number of found and expected data appears in the region where the visible energy is below $0.5\sqrt{s}$, where an important contribution from two-photon interactions and $\ell\nu\ell'\nu$ events is expected. Such events are afterwards rejected by the optimization procedure, which requires a high visible energy.

In the case of indirect decays of scalar neutrinos, the only visible decay products are the jets coming from neutralino decays. Therefore, we have derived five selections according to the neutralino mass value, reflecting the different boost and jet broadening configurations. The final selection criteria are optimized [11]

Table 4

Efficiency values (ϵ , in %) and 95% C.L. cross section upper limits (σ , in pb) for indirect decays of the supersymmetric particles, as a function of ΔM (in GeV). As an example the efficiencies at $\sqrt{s} = 206$ GeV are shown, for the most conservative choice of the couplings. At the other centre-of-mass energies they are compatible within the uncertainties. Typical relative errors on the signal efficiencies, due to Monte Carlo statistics, are between 2% and 5%. $\tilde{\chi}_m^0 \tilde{\chi}_n^0$ indicates neutralino pair-production with $m = 1, 2$ and $n = 2, \dots, 4$. The efficiencies correspond to $M_{\tilde{\chi}_m^0} + M_{\tilde{\chi}_n^0} = 206$ GeV. For indirect decays of charginos, scalar leptons and scalar quarks, the selection efficiencies correspond to a mass of 102 GeV. The upper limits on the pair-production cross sections are calculated using the data at $\sqrt{s} \geq 204$ GeV, with an integrated luminosity of 216 pb^{-1} .

Coupling	Process		ΔM									
			10	20	30	40	50	60	70	80	90	100
<i>Indirect decays</i>												
λ_{133}	$\tilde{\chi}_m^0 \tilde{\chi}_{n(n \geq 2)}^0$	ϵ	49	48	48	47	45	43	41	38	36	35
		σ	0.09	0.09	0.09	0.09	0.10	0.10	0.11	0.12	0.12	0.13
λ_{133}	$\tilde{\chi}_1^+ \tilde{\chi}_1^-$	ϵ	47	43	39	34	31	25	20	-	-	-
		σ	0.08	0.09	0.10	0.11	0.12	0.15	0.18	-	-	-
λ_{133}	$\tilde{e}_R^+ \tilde{e}_R^-$	ϵ	61	62	63	54	46	35	24	-	-	-
		σ	0.06	0.06	0.06	0.07	0.08	0.11	0.15	-	-	-
λ_{133}	$\tilde{\mu}_R^+ \tilde{\mu}_R^-$	ϵ	71	76	80	77	75	70	65	-	-	-
		σ	0.05	0.05	0.05	0.05	0.05	0.05	0.06	-	-	-
λ_{133}	$\tilde{\tau}_R^+ \tilde{\tau}_R^-$	ϵ	52	59	66	65	64	60	56	-	-	-
		σ	0.07	0.06	0.06	0.06	0.06	0.06	0.07	-	-	-
λ_{133}	$\tilde{\nu} \tilde{\nu}$	ϵ	50	49	49	43	41	39	36	-	-	-
		σ	0.07	0.07	0.07	0.08	0.08	0.09	0.10	-	-	-
λ''_{212}	$\tilde{\chi}_m^0 \tilde{\chi}_{n(n \geq 2)}^0$	ϵ	57	60	63	68	66	64	62	58	54	46
		σ	0.18	0.17	0.16	0.15	0.15	0.16	0.17	0.18	0.20	0.23
λ''_{212}	$\tilde{\chi}_1^+ \tilde{\chi}_1^-$	ϵ	65	70	69	73	72	70	71	-	-	-
		σ	0.16	0.15	0.15	0.14	0.15	0.15	0.15	-	-	-
λ''_{212}	$\tilde{e}_R^+ \tilde{e}_R^-$	ϵ	29	51	56	63	66	69	56	46	36	-
		σ	0.18	0.09	0.05	0.05	0.05	0.05	0.05	0.06	0.08	-
λ''_{212}	$\tilde{\mu}_R^+ \tilde{\mu}_R^-$	ϵ	20	28	41	49	52	55	52	42	27	-
		σ	0.10	0.05	0.05	0.05	0.05	0.05	0.05	0.06	0.09	-
λ''_{212}	$\tilde{\tau}_R^+ \tilde{\tau}_R^-$	ϵ	53	57	63	56	46	40	29	17	13	-
		σ	0.15	0.13	0.13	0.13	0.15	0.16	0.22	0.23	0.24	-
λ''_{212}	$\tilde{\nu} \tilde{\nu}$	ϵ	41	43	44	39	37	32	40	50	35	-
		σ	0.13	0.12	0.12	0.12	0.14	0.15	0.08	0.11	0.12	-
λ''_{212}	$\tilde{q} \tilde{q}$	ϵ	55	59	64	65	63	58	47	45	43	-
		σ	0.18	0.16	0.15	0.15	0.16	0.17	0.22	0.22	0.23	-

by taking into account the following variables: jet widths, $\ln(y_{34})$ and $\ln(y_{45})$, visible energy and polar angles of the missing momentum vector and of the thrust axis.

Supersymmetric partners of the right-handed leptons have no direct two-body decays via λ''_{ijk} couplings. However, when scalar leptons are lighter than $\tilde{\chi}_1^0$, the four-body decay $\tilde{\ell}_R \rightarrow \ell q \bar{q} q$ can occur [3]

Table 5

Processes considered in the λ''_{ijk} analysis and corresponding selections [11]. For masses below 50 GeV or small ΔM values not all jets in the event can be resolved. $\tilde{\chi}_m^0 \tilde{\chi}_n^0$ indicates neutralino pair-production with $m = 1, 2$ and $n = 1, \dots, 4$. For final states with neutrinos we use selections with no explicit missing energy requirement, because for those topologies \cancel{E} is small, except for the scalar neutrino decays

Direct decays		Selections
$e^+e^- \rightarrow \tilde{\chi}_m^0 \tilde{\chi}_n^0 \rightarrow$	qqqqqq	multijets
$e^+e^- \rightarrow \tilde{\chi}_1^+ \tilde{\chi}_1^- \rightarrow$	qqqqqq	multijets
Indirect decays		Selections
$e^+e^- \rightarrow \tilde{\chi}_m^0 \tilde{\chi}_{n(n \geq 2)}^0 \rightarrow$	qqqqqq qq	multijets
	qqqqqq $\ell\ell$	multijets + lepton(s)
	qqqqqq $\nu\nu$	multijets
$e^+e^- \rightarrow \tilde{\chi}_1^+ \tilde{\chi}_1^- \rightarrow$	qqqqqq qq	multijets
	qqqqqq qq $\ell\nu$	multijets + lepton(s)
	qqqqqq $\ell\ell\nu\nu$	multijets + lepton(s)
$e^+e^- \rightarrow \tilde{\ell}_R^+ \tilde{\ell}_R^- \rightarrow$	qqqqqq $\ell\ell$	6 jets + 2 ℓ
$e^+e^- \rightarrow \tilde{\nu} \tilde{\nu} \rightarrow$	qqqqqq $\nu\nu$	6 jets + \cancel{E}
$e^+e^- \rightarrow \tilde{q} \tilde{q} \rightarrow$	qqqqqq qq	multijets

providing the same final state as that resulting from indirect decays, but with virtual $\tilde{\chi}_1^0$ production. The non-resonant four-body decay is not implemented in the generator. For this reason, we use the results of the indirect decay analysis, performing a scan over all neutralino mass values up to $M_{\tilde{\ell}_R}$. The resulting lowest efficiency is conservatively quoted in the following for four-body decays. It is found in most cases for $M_{\tilde{\chi}_1^0} \simeq M_{\tilde{\ell}_R}$, as the resulting low energy lepton can not be resolved from the nearby jet. For scalar taus with masses above 70 GeV, the lowest efficiency is found for high ΔM values, as in the case of indirect decays.

5. Model-independent results

Table 6 and Table 7 show the overall numbers of candidates and expected background events for the different selections and processes, respectively. The same process may give rise to different final states (such as chargino direct decays via λ_{ijk}) or the same final state (like “multijets”) can be present as a decay product of more than one process. No

Table 6

Number of observed data (N_{data}) and expected background (N_{back}) events for the different selections in the sample at $\sqrt{s} = 192\text{--}208$ GeV. A process can give rise to several topologies, or the same topology may occur for more than a final state. The uncertainty on the expected background is due to Monte Carlo statistics. The deficit in the number of observed data in the multijet and scalar lepton λ''_{ijk} selections is correlated among the channels

Coupling	Selection	N_{back}	N_{data}
λ_{ijk}	$4\ell + \cancel{E}$	4.9 ± 0.5	6
	$(\geq 4)\ell + (\text{jets}) + \cancel{E}$	10.1 ± 0.3	10
	$2\ell + \cancel{E}$	31 ± 2	34
	6ℓ	0.85 ± 0.09	1
λ''_{ijk}	Multijets ($M_{\tilde{\chi}_1^0} = 30\text{--}40$ GeV)	146 ± 2	147
	Multijets ($M_{\tilde{\chi}_1^0} = 40\text{--}50$ GeV)	100 ± 2	109
	Multijets	446 ± 3	404
	Multijets + lepton(s) (semileptonic)	11.8 ± 0.7	9
	Multijets + lepton(s) (leptonic)	6.1 ± 0.7	5
	6 jets + 2 leptons	413 ± 2	361
	6 jets + \cancel{E}	671 ± 6	669
	4 jets	3387 ± 13	3411

Table 7

Number of observed data (N_{data}) and expected background (N_{back}) events for the different processes in the sample at $\sqrt{s} = 192\text{--}208$ GeV. Details on the selection of each topology are given in Table 6. The uncertainty on the expected background is due to Monte Carlo statistics. The deficit in the number of observed data in the neutralino, chargino and slepton λ''_{ijk} analyses is correlated among the channels

Coupling	Process	N_{back}	N_{data}
λ_{ijk}	$\tilde{\chi}_1^0 \tilde{\chi}_1^0$	4.9 ± 0.5	6
	$\tilde{\chi}_m^0 \tilde{\chi}_n^0$	14.7 ± 0.6	15
	$\tilde{\chi}_1^+ \tilde{\chi}_1^-$ (indirect)	10.1 ± 0.3	10
	$\tilde{\chi}_1^+ \tilde{\chi}_1^-$ (direct)	37 ± 3	40
	$\tilde{\ell}_R^+ \tilde{\ell}_R^-$ (indirect)	10.1 ± 0.3	10
	$\tilde{\ell}_R^+ \tilde{\ell}_R^-$ (direct)	31 ± 2	34
	$\tilde{\nu} \tilde{\nu}$	4.9 ± 0.5	6
λ''_{ijk}	$\tilde{\chi}_1^0 \tilde{\chi}_1^0$	661 ± 4	605
	$\tilde{\chi}_1^+ \tilde{\chi}_1^-$	446 ± 3	404
	$\tilde{\ell}_R^+ \tilde{\ell}_R^-$	413 ± 2	361
	$\tilde{\nu} \tilde{\nu}$	671 ± 6	669
	$\tilde{q} \tilde{q}$	3387 ± 13	3411

significant excess of events is observed. Therefore, upper limits are set on the neutralino, chargino and scalar lepton pair-production cross sections assuming direct or indirect R-parity violating decays.

In the case of λ_{ijk} couplings, upper limits are set for each process, independently of the mass value of the supersymmetric particle considered. For λ''_{ijk} couplings, upper limits are derived for each process depending on the mass range of the supersymmetric particles, since this procedure improves the sensitivity of analyses with high background level.

These limits take into account the estimated background contamination. Systematic uncertainties on the signal efficiency are dominated by Monte Carlo statistics. The typical relative error is between 2% and 5% and it is included in the calculations of the signal upper limits [26].

Tables 3 and 4 show the 95% confidence level (C.L.) upper limits on supersymmetric particle pair-production cross sections. For each mass point, all data collected at centre-of-mass energies above the production threshold are combined. For low mass values, the data at $\sqrt{s} = 189$ GeV are also used. Therefore, these upper limits should be interpreted as a limit on the luminosity-weighted average cross section.

6. Interpretation in the MSSM

In the MSSM framework, neutralino and chargino masses, couplings and cross sections depend on the gaugino mass parameter, M_2 , the higgsino mass mixing parameter, μ , the ratio of the vacuum expectation values of the two Higgs doublets, $\tan\beta$, and the common mass of the scalar particles at the GUT scale, m_0 . The results presented in this section are obtained by performing a scan in the ranges: $0 \leq M_2 \leq 1000$ GeV, -500 GeV $\leq \mu \leq 500$ GeV, $0 \leq m_0 \leq 500$ GeV and $0.7 \leq \tan\beta \leq 40$. They do not depend on the value of the trilinear coupling in the Higgs sector, A .

6.1. Mass limits from scalar lepton and scalar quark searches

For scalar lepton and scalar quark pair-production, mass limits are derived by direct comparison of the 95% C.L. cross section upper limits with the scalar

particle pair-production cross sections, which depend on the scalar particle mass.

We assume no mixing in the scalar lepton sector. Scalar electron and scalar electron neutrino pair-production have an additional contribution from the t -channel exchange of a neutralino or chargino, whose mass spectrum depends on the MSSM parameters. In this case the mass limits are derived at a given value of $\tan\beta$ and μ , here chosen to be $\tan\beta = \sqrt{2}$ and $\mu = -200$ GeV. For scalar quarks, mixing is taken into account for the third generation. The cross section depends on the scalar quark mass and on the mixing angle θ_{LR} . For $\sqrt{s} = 189$ –208 GeV the production cross section for scalar top pairs is minimal for $\cos\theta_{LR} \sim 0.51$ and for scalar bottom pairs for $\cos\theta_{LR} \sim 0.36$. These values are conservatively used in this analysis.

Figs. 3 and 4 show the excluded 95% C.L. contour for different scalar lepton and scalar quark masses, as a function of the neutralino mass. Indirect decays of the scalar leptons dominate over direct ones in the region with $\Delta M > 2$ GeV. For $0 \leq \Delta M < 2$ GeV 100% branching ratio either into direct or indirect decays is assumed and the worst result is shown. In the negative ΔM region only direct decays contribute. For λ''_{ijk} direct decays of the scalar leptons we quote the results from four-body processes. The 95% C.L. lower mass limits are shown in Table 8, for both direct and indirect decays.

6.2. Mass limits from combined analyses

A point in the MSSM parameter space is excluded if the total number of expected events is greater than the combined upper limit at 95% C.L. on the number of signal events. Neutralino, chargino, scalar lepton and scalar quark analyses are combined since several processes can occur at a given point. Gaugino and scalar mass unification at the GUT scale is assumed. The constraints from the L3 lineshape measurements at the Z pole [25] are also taken into account [11]. We derive lower limits at 95% C.L. on the neutralino, chargino and scalar lepton masses, as detailed in Table 9.

Fig. 5 shows the 95% C.L. lower limits on neutralino and scalar lepton masses as a function of $\tan\beta$. The $\tilde{\chi}_1^0$ and $\tilde{\chi}_2^0$ mass limits are shown for $m_0 = 500$ GeV and the $\tilde{\ell}_R$ ones for $m_0 = 0$. These values

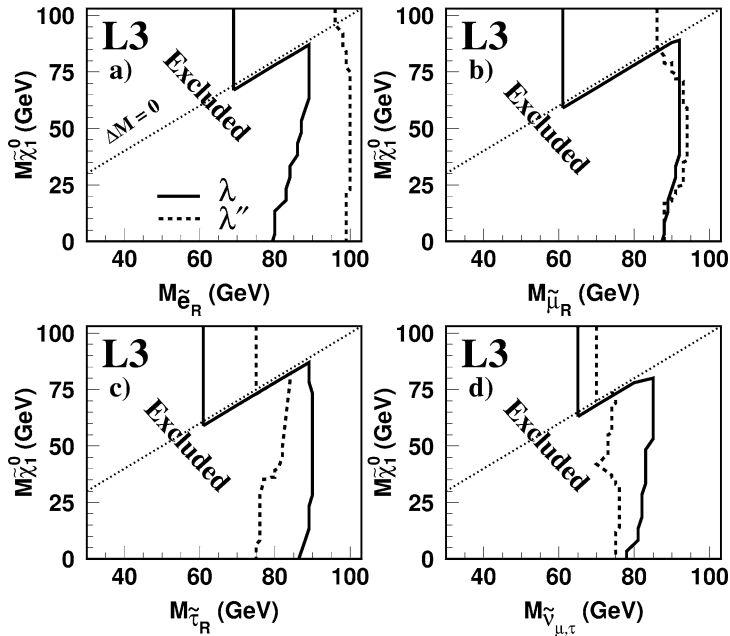


Fig. 3. MSSM exclusion contours, at 95% C.L., for the masses of (a) \tilde{e}_R , (b) $\tilde{\mu}_R$, (c) $\tilde{\tau}_R$ and (d) $\tilde{\nu}_{\mu,\tau}$ as a function of the neutralino mass. The solid and dashed lines, show the λ and λ'' exclusion contours, respectively. The dotted line corresponds to $\Delta M = 0$. For $\Delta M < 0$, above this line, the exclusion contours from direct decays are shown.

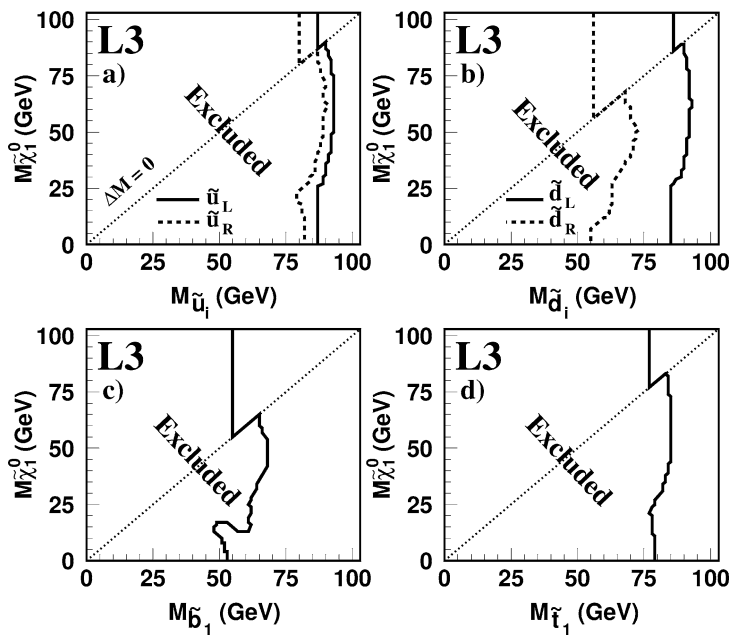


Fig. 4. MSSM exclusion contours, at 95% C.L., for the masses of (a) up-type (b) down-type scalar quarks (c) \tilde{b}_1 and (d) \tilde{t}_1 as a function of the neutralino mass, for λ'' coupling. The solid and dashed lines show the exclusion contours for (a) \tilde{u}_L, \tilde{u}_R and (b) \tilde{d}_L, \tilde{d}_R , respectively. For $\Delta M < 0$, above the dotted line, the exclusion contours from direct decays are shown.

Table 8

Lower limits at 95% C.L. on the masses of the scalar leptons and scalar quarks. The limits result from direct comparison of the 95% C.L. cross section upper limits with the scalar particle pair-production cross sections. \bar{u}_R , \bar{u}_L , \bar{d}_R and \bar{d}_L refer to any type of up and down supersymmetric partners of the right-handed and left-handed quarks. \tilde{t}_1 and \tilde{b}_1 limits are quoted in the case of minimal production cross section. For λ''_{ijk} direct decays of scalar leptons we refer to four-body processes

Coupling	Mass limit (GeV)										
	$M_{\tilde{e}_R}$	$M_{\tilde{\mu}_R}$	$M_{\tilde{\tau}_R}$	$M_{\tilde{\nu}_{\mu,\tau}}$	$M_{\tilde{\nu}_e}$	$M_{\tilde{u}_R}$	$M_{\tilde{u}_L}$	$M_{\tilde{d}_R}$	$M_{\tilde{d}_L}$	$M_{\tilde{t}_1}$	$M_{\tilde{b}_1}$
λ_{ijk} (direct)	69	61	61	65	95	–	–	–	–	–	–
λ_{ijk} (indirect)	79	87	86	78	99	–	–	–	–	–	–
λ''_{ijk} (direct)	96	86	75	70	99	80	87	56	86	77	55
λ''_{ijk} (indirect)	96	86	75	70	99	79	87	55	86	77	48

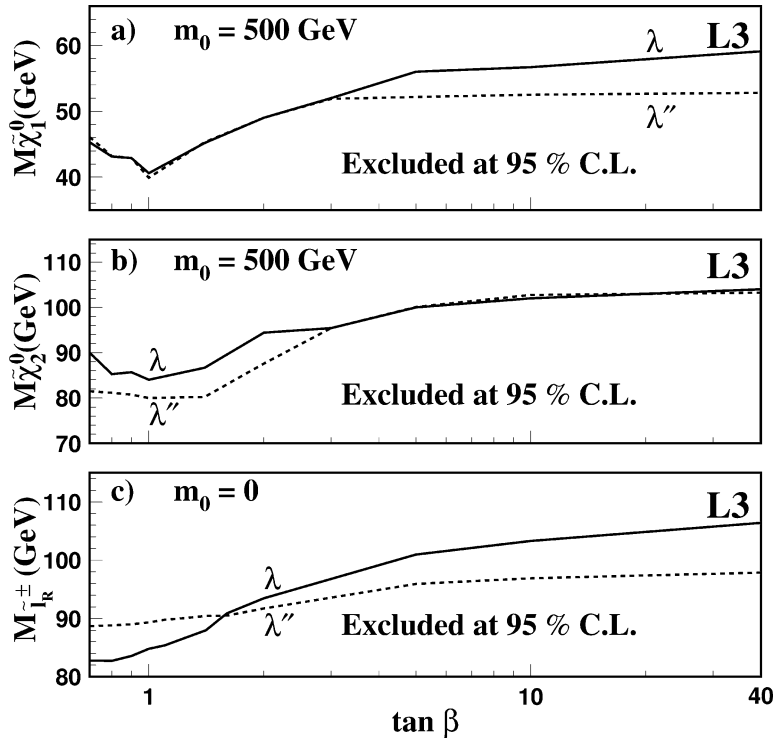


Fig. 5. MSSM mass limits from combined analyses. The solid and dashed lines, labelled with the corresponding coupling, show the 95% C.L. lower limits on the masses of (a) $\tilde{\chi}_1^0$, (b) $\tilde{\chi}_2^0$ and (c) \tilde{e}_R , as a function of $\tan \beta$, for $0 \leq M_2 \leq 1000$ GeV and -500 GeV $\leq \mu \leq 500$ GeV. $m_0 = 500$ GeV in (a) and (b) and $m_0 = 0$ in (c). For those values of m_0 the global minima on the mass limit are obtained.

of m_0 correspond to the absolute minima from the complete scan on M_2 , μ , m_0 and $\tan \beta$. The chargino mass limit is almost independent of $\tan \beta$, and is close to the kinematic limit for any value of $\tan \beta$ and m_0 . For high m_0 values, neutralino and scalar lepton pair-production contributions are suppressed and the mass

limits are given mainly by the chargino exclusion. For low m_0 , the possible production of intermediate real scalar particles does not affect our limits.

For $0 \leq m_0 < 50$ GeV and $1 \leq \tan \beta < 2$, the lightest scalar lepton, the supersymmetric partner of the right-handed electron, can be the LSP. Therefore, in

Table 9

Lower limits at 95% C.L. on the masses of the supersymmetric particles considered in this analysis. The limits result from combined analysis at each MSSM point and from a global scan in the parameter space, as detailed in Section 6. The limits on $M_{\tilde{\ell}_R}$ hold for \tilde{e}_R , $\tilde{\mu}_R$ and $\tilde{\tau}_R$

Coupling	Mass limit (GeV)					
	$M_{\tilde{\chi}_1^0}$	$M_{\tilde{\chi}_2^0}$	$M_{\tilde{\chi}_3^0}$	$M_{\tilde{\chi}_1^\pm}$	$M_{\tilde{\ell}_R}$	$M_{\tilde{\nu}}$
λ_{ijk}	40.2	84.0	107.2	103.0	82.7	152.7
λ''_{ijk}	39.9	80.0	107.2	102.7	88.7	149.0

this region only the scalar lepton analysis contributes to the limit on the scalar lepton mass. For higher values of $\tan\beta$, $\tilde{\chi}_1^0$ is the LSP and the lower limit on the scalar lepton mass is mainly given by the $\tilde{\chi}_1^0\tilde{\chi}_1^0$ exclusion contours. The absolute limit on $M_{\tilde{\ell}_R}$ is found at $\tan\beta = 0.8$ in the case of λ_{ijk} and at $\tan\beta = 0.7$ for λ''_{ijk} . The difference in the limits is due to the lower cross section upper limit of λ''_{ijk} for scalar lepton direct decays, since the limit on $M_{\tilde{\ell}_R}$ is found when the $\tilde{\ell}_R$ is the LSP. The same limits are obtained without the assumption of a common scalar mass at the GUT scale. For λ_{ijk} the bounds on the scalar lepton masses are found in the case in which the $\tilde{\ell}_R$ is the LSP. For λ''_{ijk} the limits are found when the $\tilde{\ell}_R$ and $\tilde{\chi}_1^0$ are nearly degenerate in mass. In both cases, the neutralino analyses give the main contribution to the exclusion in the regions of the parameter space around the limit. The remaining sensitivity is due to searches for direct slepton decays via λ_{ijk} . As these searches are equally sensitive to scalar electron, muon or tau signals, as shown in Table 3, the limits are unchanged. The scalar neutrino mass limit is also mainly due to neutralino exclusions, resulting in a 95% C.L. lower limit on the scalar neutrino mass above the kinematic limit.

The search for R-parity violating decays of supersymmetric particles reaches at least the same sensitivity as in the R-parity conserving case [27]. Therefore, the supersymmetry limits obtained at LEP are independent of R-parity conservation assumptions.

References

- [1] A review can be found for example in: H.E. Haber, G.L. Kane, Phys. Rep. 117 (1985) 75.
- [2] C.S. Aulakh, R.N. Mohapatra, Phys. Lett. B 119 (1982) 136; F. Zwirner, Phys. Lett. B 132 (1983) 103; L.J. Hall, M. Suzuki, Nucl. Phys. B 231 (1984) 419; For a recent review and a reference to the literature: H. Dreiner, An introduction to explicit R-parity violation, in: G.L. Kane (Ed.), Perspectives on Supersymmetry, World Scientific, Singapore, 1998, hep-ph/9707435.
- [3] R. Barbieri, A. Masiero, Nucl. Phys. B 267 (1986) 679.
- [4] L3 Collaboration, M. Acciarri et al., Phys. Lett. B 471 (1999) 280; L3 Collaboration, M. Acciarri et al., Phys. Lett. B 471 (1999) 308; L3 Collaboration, M. Acciarri et al., Phys. Lett. B 472 (2000) 420, and references therein.
- [5] S. Weinberg, Phys. Rev. D 26 (1982) 287; G. Bhattacharyya, P.B. Pal, Phys. Rev. D 59 (1999) 097701.
- [6] Particle Data Group, D.E. Groom et al., Eur. Phys. J. C 15 (2000) 1.
- [7] ALEPH Collaboration, R. Barate et al., Eur. Phys. J. C 12 (2000) 183; DELPHI Collaboration, P. Abreu et al., Phys. Lett. B 485 (2000) 45; L3 Collaboration, M. Acciarri et al., Phys. Lett. B 489 (2000) 81; OPAL Collaboration, G. Abbiendi et al., Eur. Phys. J. C 6 (1999) 1.
- [8] ALEPH Collaboration, R. Barate et al., Eur. Phys. J. C 19 (2001) 415.
- [9] S. Dawson, Nucl. Phys. B 261 (1985) 297.
- [10] L3 Collaboration, M. Acciarri et al., Phys. Lett. B 459 (1999) 354.
- [11] L3 Collaboration, M. Acciarri et al., Eur. Phys. J. C 19 (2001) 397.
- [12] ALEPH Collaboration, D. Buskulic et al., Phys. Lett. B 349 (1995) 238; ALEPH Collaboration, D. Buskulic et al., Phys. Lett. B 384 (1996) 461; ALEPH Collaboration, R. Barate et al., Eur. Phys. J. C 4 (1998) 433; ALEPH Collaboration, R. Barate et al., Eur. Phys. J. C 7 (1999) 383; ALEPH Collaboration, R. Barate et al., Eur. Phys. J. C 13 (2000) 29; DELPHI Collaboration, P. Abreu et al., Eur. Phys. J. C 13 (2000) 591; DELPHI Collaboration, P. Abreu et al., Phys. Lett. B 487 (2000) 36; DELPHI Collaboration, P. Abreu et al., Phys. Lett. B 500 (2001) 22; DELPHI Collaboration, P. Abreu et al., Phys. Lett. B 502 (2001) 24; OPAL Collaboration, G. Abbiendi et al., Eur. Phys. J. C 11 (1999) 619; OPAL Collaboration, G. Abbiendi et al., Eur. Phys. J. C 12 (2000) 1.
- [13] L3 Collaboration, B. Adeva et al., Nucl. Instrum. Methods A 289 (1990) 35;

- J.A. Bakken et al., Nucl. Instrum. Methods A 275 (1989) 81;
O. Adriani et al., Nucl. Instrum. Methods A 302 (1991) 53;
B. Adeva et al., Nucl. Instrum. Methods A 323 (1992) 109;
K. Deiters et al., Nucl. Instrum. Methods A 323 (1992) 162;
F. Beissel et al., Nucl. Instrum. Methods A 332 (1993) 33;
M. Chemarin et al., Nucl. Instrum. Methods A 349 (1994) 345;
M. Acciarri et al., Nucl. Instrum. Methods A 351 (1994) 300;
G. Basti et al., Nucl. Instrum. Methods A 374 (1996) 293;
I.C. Brock et al., Nucl. Instrum. Methods A 381 (1996) 236;
A. Adam et al., Nucl. Instrum. Methods A 383 (1996) 342.
- [14] S. Katsanevas, S. Melachroinos, in: G. Altarelli, T. Sjöstrand, F. Zwirner (Eds.), Proceedings of the Workshop “Physics at LEP 2”, Vol. 2, 1996, p. 328, CERN 96-01;
SUSYGEN 2.2, S. Katsanevas, P. Morawitz, Comput. Phys. Commun. 112 (1998) 227.
- [15] T. Sjöstrand, Preprint CERN-TH/7112/93 (1993), revised August 1995;
T. Sjöstrand, Comput. Phys. Commun. 82 (1994) 74;
T. Sjöstrand, hep-ph/0001032.
- [16] S. Jadach et al., Phys. Lett. B 390 (1997) 298.
- [17] KK2F Version 4.12 is used;
S. Jadach, B.F.L. Ward, Z. Wąs, Comput. Phys. Commun. 130 (2000) 260.
- [18] PHOJET Version 1.05 is used;
R. Engel, Z. Phys. C 66 (1995) 203;
R. Engel, J. Ranft, Phys. Rev. D 54 (1996) 4244.
- [19] F.A. Berends, P.H. Daverveldt, R. Kleiss, Nucl. Phys. B 253 (1985) 441.
- [20] KORALW Version 1.33 is used;
M. Skrzypek et al., Comput. Phys. Commun. 94 (1996) 216;
M. Skrzypek et al., Phys. Lett. B 372 (1996) 289.
- [21] F.A. Berends, R. Kleiss, R. Pittau, Comput. Phys. Commun. 85 (1995) 437.
- [22] GEANT Version 3.15 is used;
R. Brun et al., preprint CERN DD/EE/84-1 (1984), revised 1987.
- [23] H. Fesefeldt, RWTH Aachen Report PITHA 85/2 (1985).
- [24] S. Catani et al., Phys. Lett. B 269 (1991) 432;
S. Bethke et al., Nucl. Phys. B 370 (1992) 310;
N. Brown, W.J. Stirling, Z. Phys. C 53 (1992) 629.
- [25] L3 Collaboration, M. Acciarri et al., Eur. Phys. J. C 16 (2000) 1.
- [26] R.D. Cousins, V.L. Highland, Nucl. Instrum. Methods A 320 (1992) 331.
- [27] B. Clerbaux, P. Azzurri, in: Proceedings of the International Europhysics Conference on High Energy Physics, July 12–18, Budapest, Hungary, 2001.